Optimal slot numbers combination for magnetic noise reduction in variable-speed induction motors

J. Le Besnerais, V. Lanfranchi, M. Hecquet, and P. Brochet, *Member, IEEE*

***Abstract*— Numerous empirical rules have been established in order to rightly choose the number of stator and rotor slots and limit the audible magnetic noise level radiated by induction machines. However, these rules never take into account the stator natural frequencies neither the fact that the motor is run at variable speed.**

In this article, a fast simulation tool of the variable-speed magnetic noise emitted by induction machines, based on fully analytical models, is presented. On the ground of these models, the analytical expression of main magnetic vibrations due to slotting reluctance harmonics are derived and experimentally validated, confirming the prime importance of slot combination in magnetic noise radiation.

Some simulations are then run on a 700 W squirrel-cage motor in order to quantify the noise emitted by all possible combination of slot numbers in two and three pole pairs cases, including odd slot numbers. The obtained database efficiently replaces the old emperical rules on slot combination numbers and helps designing quiet induction motors. Similar database can be built for other power ranges.

***Index Terms*— Induction machine, magnetic noise, slot number, natural frequencies.**

NOMENCLATURE

b_r	Rotor slot opening width
b_s	Stator slot opening width
D_r	Rotor stack outer diameter
D_s	Stator stack inner diameter
f_{max}	Maximum supply frequency
f_n	n-th circumferential mode natural frequency
f_R	Rotor mechanical frequency ($f_R = f_s(1-s)/p$)
f_s	Fundamental stator supply frequency
m	Spatial order of a force harmonic
n	n-th stator circumferential mode
p	Number of pole pairs
q_s	Number of stator phases
s	Fundamental slip
Z_r	Number of rotor slots
Z_s	Number of stator slots
μ_0	Air-gap magnetic permeability

I. INTRODUCTION

Manuscript received the 12th of February, 2009. This work was supported in part by the French Agence De l'Environnement et de la Maîtrise de l'Energie.

J. Le Besnerais is with the Laboratoire d'Electrotechnique et d'Electronique de Puissance (L2EP), Ecole Centrale de Lille, FRANCE (e-mail:jean.le_besnerais@centraliens.net, website:http://l2ep.univ-lille1.fr/pagesperso/lebesnerais/).

V. Lanfranchi is with the LEC (Laboratoire d'Electromécanique de Compiègne), UTC, Compiègne, FRANCE (e-mail: vincent.lanfranchi@utc.fr).

M. Hecquet and P. Brochet are also with the L2EP (e-mail: michel.hecquet@ec-lille.fr and pascal.brochet@ec-lille.fr).

THe strong vibro-acoustic influence of the slot numbers combination used in squirrel-cage induction machines was experimented at the early beginning of the twentieth century. Consequently, some researchers started to look for some general rules to decrease these motor noise and vibrations mainly due to Maxwell air-gap magnetic forces, the first one being Kron [1] in 1908. During the following decades, other attempts to infer some general rules from the numerous experiments run on different motors were done ; an exhaustive list of these laws can be found in Timar book [2] in 1989 (for instance $0.75Z_s \leq Z_r < Z_s$).

Nevertheless, these rules have major drawbacks: firstly, they are continuous although magnetic resonances come from discrete harmonic phenomena, as shown in section II ; secondly, they are independent of the motor natural frequencies and motor maximal supply frequency f_s, which sizes the frequency range of magnetic exciting forces, so they cannot correctly account for resonance phenomena ; finally, some of them are also based on the limitation of electromagnetic torque pulsations, whose correlation with the audible magnetic noise phenomenon has not been clearly demonstrated yet. Some new reliable design rules have therefore to be established on several ranges of stator mechanical structure and motor maximum speed.

In this article is first detailed the phenomenon of audible magnetic noise generation. Then, a fully analytical model of the induction machine electromagnetic and vibro-acoustic behavior, called DIVA [3], [4], is quickly presented. On the ground of these models are detailed the analytical expressions of the main magnetic vibration waves due to radial air-gap Maxwell forces linked with slotting harmonics, in terms of rotation velocity and number of nodes. These expressions are experimentally validated by visualizing a stator deflection shape (Operational Deflection Shape) at some given frequencies. Finally, a simulation method is presented in order to establish some new low-noise design rules for the slot numbers combinations. This method is applied to a 700 W, 10 cm external diameter squirrel-cage induction machine, and the best slot numbers are given.

II. MAGNETIC NOISE PHENOMENON

Magnetic forces can be classified in magnetostrictive forces and Maxwell forces. Magnetostrictive vibrations rather affect low frequencies, and especially the component at twice the fundamental stator frequency where it can even be in counter-phase of Maxwell forces in two-pole machines [5], [6]. They are neglected in this paper that focuses on the reduction of high-pitch acoustic noise due to Maxwell forces.

The global effect of Maxwell forces on the stator can be brought to a Maxwell pressure distribution in the air-gap [7]. This pressure P_M is purely radial on stator teeth, it can be approximated by [8], [2], [9]

$$P_M = B_g^2/(2\mu_0) \tag{1}$$

where B_g is the radial air-gap flux density. Assuming that the rotor is not skewed, and neglecting end-effects, this force distribution is independent of the axial direction and can therefore only excite some circumferential modes of the stator, which can be modeled by an equivalent ring as a first approximation [2], [10]. Each of these circumferential modes is associated to a number ($n = 0, 1, 2, 3, 4, ...$) and a natural frequency f_n (see example of $n = 2$ in Fig. 1).

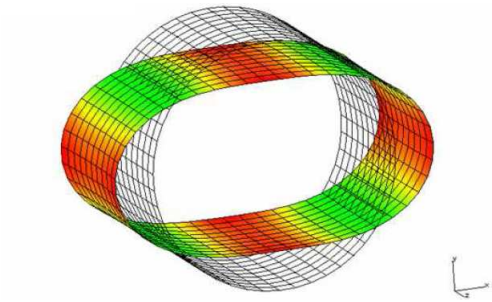

Fig. 1. Example of the elliptical circumferential mode ($n = 2$) of a cylindrical shell (structural finite element method).

Developing the magnetic pressure (1) in two-dimensional Fourier series, it can be expressed as an infinite sum of progressive force waves of time frequency f and space frequency m:

$$P_M(t, \alpha_s) = \sum_{m,f} A_{mf} \cos(2\pi f t - m\alpha_s + \phi_{mf}) \tag{2}$$

m is also called a spatial order, it corresponds to half the number of nodes i.e. zero magnitude points (see Fig. 2 example for $m = 2$ where there are four nodes). Note that such a force wave do not rotate at f frequency, but at f/m frequency.

A magnetic resonance, i.e. large vibration and acoustic levels, can then occur at two conditions as analytically proven in [11]:

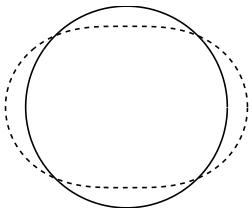

Fig. 2. Example of a 2-order ($m = 2$) rotating force wave coming from the Fourier series development of radial air-gap Maxwell forces distribution. The fundamental difference with the deflection shape of the stator elliptical mode in Fig. 1 is the fact that the exciting force nodes are rotating, whereas the mode deflection nodes are steady, fixed according to the maximal stiffness points of the structure.

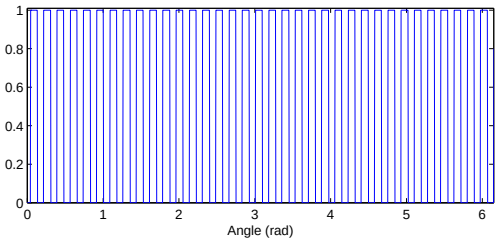

Fig. 3. C_s function marking the location of stator slot openings along the air-gap.

1) the order m of the force wave must be the same as the circumferential mode number n of the stator ring ($m = n$)
2) the frequency of the force wave must be the same as the frequency of the natural frequency of the stator mode under consideration ($f = f_n$)

In variable-speed motors, the frequency match condition 2) is more easily satisfied as the frequencies of magnetic forces due to fundamental current vary proportionally to the supply frequency f_s, and therefore sweep a wide frequency range during starting and braking. There exist an infinite number of force harmonics, but the magnitude of the vibration waves that they generate are inversely proportional to m^4 [9], so that only the lowest spatial orders forces lead to significant vibration and noise (0 to 4 for induction motors up to several hundreds of kW).

III. Magnetic Noise Prediction

A. Electromagnetic model

In order to predict magnetic noise resonances, one must therefore analytically calculate the Fourier development of P_M. This requires an analytical model of the air-gap radial flux density distribution, for instance a permeance / magnetomotive force (mmf) decomposition [12]. Neglecting the rotor mmf that is generally much lower than stator mmf and do not introduce new noisy resonances [13], this decomposition can be written as [14]

$$B_g = \Lambda f_{mm}^s = \frac{\mu_0}{g_f} f_{mm}^s \tag{3}$$

where g_f is the air-gap "fictitious width", i.e. the mean length of flux density lines along the air-gap, and f_{mm}^s is the stator magnetomotive force (mmf). Considering that the stator mmf is nearly sinusoidal, only the Fourier series of permeance must be determined. This can be done approximating it by a crenel function, assuming that a fixed value d_s^f and d_r^f for the mean flux line length entering into stator and rotor slots. This way, g_f can be written as

$$g_f(t, \alpha_s) = g + d_s^f C_s(\alpha_s) + d_r^f C_r(t, \alpha_s) \tag{4}$$

where C_s and C_r are boolean functions that mark the stator and rotor slot openings locations (see Fig. 3). [15] expresses fictitious depths that are proportional to slot openings ($d_s^f = b_s/5$ and $d_r^f = b_r/5$). Note that these fictitious slot depths

do not depend on the real slot depth, but on the slot opening width, so that for closed rotor slots $d_r^f = 0$.

Now that the permeance function is fully defined, it can be developed in Fourier series in order to express all Maxwell force harmonics. Its Fourier development gives [15]:

$$\begin{aligned}\Lambda = \Lambda_0 &+ \sum_{k_s=1}^{\infty} \Lambda_{k_s} \cos(k_s Z_s \alpha_s) \\ &+ \sum_{k_r=1}^{\infty} \Lambda_{k_r} \cos\left(k_r Z_r(\alpha_s - \alpha_r)\right) \\ &+ \frac{1}{2} \sum_{k_s=1}^{\infty} \sum_{k_r=1}^{\infty} \Lambda_{k_s k_r} \{\cos((k_s Z_s - k_r Z_r)\alpha_s + k_r Z_r \alpha_r) \\ &+ \cos((k_s Z_s + k_r Z_r)\alpha_s - k_r Z_r \alpha_r)\} \quad (5)\end{aligned}$$

where α_r stands for a rotor bar angular position:

$$\alpha_r(t) = \frac{2\pi f_s}{p}(1-s)t = 2\pi f_R t \quad (6)$$

The detailed expression of coefficients $\Lambda_0, \Lambda_{k_s}, \Lambda_{k_r}$ and $\Lambda_{k_s k_r}$ can be found in [15], [4]. $\Lambda_{k_{s/r}}$ are inversely proportional to $k_{s/r}$, so that the higher k_r and k_s are, the lower are their associated permeance harmonics. Another important fact is that $\Lambda_{k_s k_r}$ is much smaller than $\Lambda_{k_{s/r}}$, so it will be neglected in this paper. Note that it cannot be neglected when considering saturation effect on noise [16].

Now that the full Fourier development of permeance function has been determined, one can easily find the expression of all the air-gap radial flux density harmonics, and then Maxwell force harmonics resulting from all possible combinations of flux density harmonics. This gives numerous pressure waves whose exhaustive list can be found in [13]. However, only the lowest spatial order ones are significant, and some of them have very low magnitude as they come from the multiplication of low magnitude harmonics. Neglecting them, one obtains the main force harmonics given in Table I.

TABLE I

PURE SLOTTING FORCE LINES EXPRESSION.

	Frequency f	Spatial order m
F_{slot}^{-}	$f_s(k_r Z_r(1-s)/p - 2)$	$k_r Z_r - k_s Z_s - 2p$
F_{slot}^{0}	$f_s(k_r Z_r(1-s)/p)$	$k_r Z_r - k_s Z_s$
F_{slot}^{+}	$f_s(k_r Z_r(1-s)/p + 2)$	$k_r Z_r - k_s Z_s + 2p$

They can be grouped in three infinite families. They correspond to Maxwell harmonics due to permeance fluctuations along the air-gap (slotting effect) when feeding the machine with sinusoidal currents: they theoretically cancel if rotor or stator slots are fully closed. These forces remain unchanged when feeding the induction machine with Pulse-Width Modulation (PWM).

In Table I, it is clear that Z_r and Z_s have a strong influence on magnetic noise: Z_s and Z_r change the spatial orders of the exciting force harmonics, and Z_r changes their frequencies. Z_r is therefore a degree of freedom with higher impact than Z_s, which goes in the right sense as it is less expensive to manufacture a new squirrel-cage rotor than a stator that requires rewinding the machine.

We can also see that the phenomenon is discrete: if a given (Z_r, Z_s) combination can lead to a low order m force harmonic with very high magnitude (e.g. $k_r = k_s = 1$), a very slight change of Z_r can make this low order harmonic disappear or have a very low magnitude.

B. Vibro-acoustic model

The vibro-acoustic model approximates the stator as an equivalent ring, so that its static deflections and circumferential modes natural frequencies f_n can be analytically expressed. The dynamic behavior of the stator structure is modeled using an empirical law for damping coefficients [10]. The acoustic power is then computed using the expression of the radiation factor of an infinite cylinder or a sphere according to the stator dimensions [17].

A more detailed description of this model can be found in [13], [4].

C. Validation

The model has been validated at different stages (flux density, vibration, sound power level) by numerical methods and/or tests [3], [13], [4], [18], [19].

The natural frequencies computation has been validated with finite element method (FEM), and hammer shock experimental modal analysis [4]. These validation results are recalled in Table II.

TABLE II

STATOR NATURAL FREQUENCIES f_n COMPUTATION (HZ) USING DIFFERENT METHODS. OR: OUT OF RANGE, ID: INDEFINITE.

n	2-D FEM	Hammer shock	DIVA
0	14656	OR	14859
1	ID	1200	1234
2	2364	2400	2485
3	6473	6100	6415
4	11898	11700	12065

The expressions of modes and frequencies of Table I have been validated experimentally by visualizing some stator deflection shapes at different frequencies. Some accelerometers have been placed along the outer median circumference of the stator stack, and the acceleration signals have been post-processed in Pulse Labshop® software. Test-bench motor parameters are given in Table III.

TABLE III

MOTOR PARAMETERS.

Number of pole pairs p	2
Number of stator slots Z_s	27
Number of rotor slots Z_r	21
Output nominal power (W)	700
Maximum supply frequency (Hz)	90
Stator stack outer diameter (mm)	204
Stator stack inner diameter (mm)	63
Stator stack length (mm)	80
Airgap width (mm)	0.2

As an example, we can see that for $k_r = 5$ and $k_s = 4$, a Maxwell force harmonic with mode $5 \times 21 - 4 \times 27 = -3$ occurs at frequency $f_s(105(1-s)/2)$; in agreement with analytical predictions, the operational deflection shape of the stator at this frequency is a rotating vibration wave of order 3 as shown in Fig. 4.

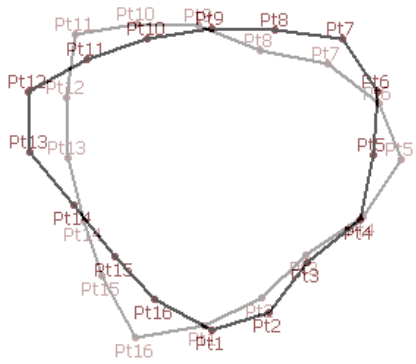

Fig. 4. Experimental stator deflection shape at two successive moments at frequency $f_s(105(1-s)/2)$.

IV. Magnetic noise reduction

A. Low-noise analytical rule

In order to avoid resonances between slotting magnetic forces of Table I and circumferential modes of the stator during starting (the stator supply frequency going from 0 to f_{max} Hz), the following condition must be fulfilled:

$$f_{max}(k_r Z_r(1-s)/p+2\gamma) < f_n, n = |k_r Z_r - k_s Z_s + \gamma 2p| \quad (7)$$

for $\gamma \in [-1, 0, 1]$, especially when n is low (0 to 4) and k_r and k_s are low (1 to 5). The slot numbers can be chosen according to this rule, with the help of a simple computer program. However, how can the designer choose between a (Z_r, Z_s) solution generating small but numerous resonances, and a (Z_r, Z_s) solution generating a strong but single resonance ? To quantitatively classify all the possible solutions in term of acoustic noise, simulation is therefore necessary.

B. Low-noise slot combination database

The analytical model that has been described in section III gives a fast Matlab® simulation tool called DIVA that can compute the motor magnetic sound power level in only a few seconds on a 2 GHz laptop. All the slot number combinations can exhaustively be tested at variable-speed in order to establish a low-noise slot combination database, instead of trying to define general analytical rules.

On the ground of the test motor described in Table III, some virtual four-pole motors with all possible combinations of Z_s and Z_r from 10 to 50, including odd slot numbers, have been run from 0 to 2700 rpm. As Z_s values are not always proportional to $2pq_s$, this applies to both integral and fractional-slot stator windings. These motors were simulated with sinusoidal supply and sinusoidal mmf in order to simulated pure slotting noise as defined in Table I.

In all cases, the stator current has been forced to the same value, in order to have a magnetic excitation of constant magnitude. However, slotting permeance harmonics magnitude also depends on slotting ratios $sl_{r/s}$ [15] defined as

$$sl_s = 1 - \frac{b_s}{\tau_s} \quad sl_r = 1 - \frac{b_r}{\tau_r} \quad (8)$$

where

$$\tau_s = \pi D_s / Z_s \quad \tau_r = \pi D_r / Z_r \quad (9)$$

To keep these slotting ratios constant when changing the number of stator and rotor slots, the products $Z_r b_r$ and $Z_s b_s$ have also been forced to be constant (otherwise, increasing the number of slots would have reduced the slot openings, and reduced the magnetic force lines magnitude). This way, the computed noise levels only reflect the resonances effect of the slot combination, and this independently of the slots geometry and winding type. Such a methodology allows to decomposing low-noise guidelines applying to the slot combination numbers from the ones applying to the slot geometries.

The resulting database is a 50 by 50 table that contains the maximum and the average magnetic noise level radiated by each motor during starting phase. Some more data has been recorded during simulations, such as the number of resonances, and the excited stator circumferential modes for each slot combination.

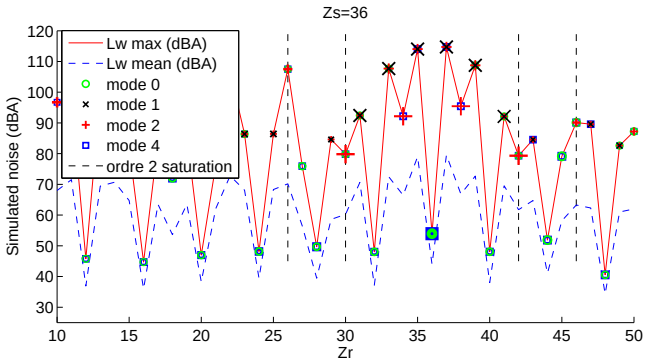

Fig. 5. Evolution of a $Z_s = 36$ stator-slot motor magnetic sound power level (average and maximum levels during starting) in function of the number of rotor slots Z_r.

An example of the database obtained on motor M1 is displayed in Fig. 5 for $Z_s = 36$, $p = 2$. In that figure, one can see that the noise level greatly changes with the number of rotor slots: the phenomenon is discrete, for instance changing from 38 or 39 to $Z_r = 40$ rotor slots completely changes the noise level. Some other information has been recorded during simulations, and illustrated in Fig. 5. For instance, the participation of each stator mode to the global noise level shows that $Z_r = 38$ is noisy because it excites the stator elliptical mode ($n = 2$). Similarly, it can be observed that mode number 1 is only excited when the rotor slot number is odd, which is clear from Table I. Finally, some information on noise due to saturation has been also displayed: saturation

modifies the radial air-gap flux density shape, adding new harmonics that can generate additional resonances [16]. This effect has not been included in simulations because this work aims at studying the effect of slot numbers combination on noise and vibrations independently of the slot shapes that size the exciting slotting force harmonics, as well as saturation force harmonics. Some slot combinations can create some saturation harmonics of order 2, which are especially dangerous when they excite the stator elliptical mode: these slot combinations have been indicated by a dashed line in Fig. 5 so that the designer keeps in mind that this kind of combination can possibly lead to strong resonances due to saturation.

The full 250 element table obtained with these simulations cannot be shown in this paper, so the quietest combinations have been selected and are presented in Table IV. They have been classified for each given stator slot number, because the squirrel-cage rotor is more easily manufactured than the stator that comprises winding. The rotor slot numbers are presented by increasing noise order, but this classification is rather subjective, especially because two different objectives are considered at the same time (average and maximum noise during starting): a weight must be fixed between both objectives to quantitatively and objectively sort them. It is therefore advised to refer to the table full version of this work in [13]. In this Table, the combination $Z_r = Z_s$ has been removed, although it systematically belongs to the quietest ones, because it creates high synchronous parasite torques [20]. Other combinations are unrealistic (e.g. when $Z_r \gg Z_s$), but they are all shown so that some general rules can be more easily inferred.

Several important conclusions can be drawn from these simulations. Firstly, when Z_s is odd (resp. even), which is the case for fractional-slot windings, there exist some quiet combinations with both even and odd Z_r. Secondly, some combinations are clearly less noisy than others: it is the case of Z_s that are multiples of 4, with Zr also multiples of 4. Indeed if $Z_s = 2pq_s$ and $Z_r = 2pq_r$, the slotting force harmonics have spatial orders of the form

$$k_r Z_r - k_s Z_s + \gamma 2p = 2p(k_r q_r - k_s q_s + \gamma) \qquad (10)$$

which means for $p = 2$ that they have orders 0, 4, 8 etc: slotting forces cannot excite the most dangerous stator mode, the elliptical one.

Note that Table IV results must be used with special care: it does not account for saturation effects, nor slot geometry influence, and it is only valid for four-pole motors whose natural frequencies are close to ones of Table II, and whose maximal supply frequency during starting is close to 90 Hz.

Ideally, the designer should first choose the slot numbers using a similar study as this one in order to avoid strong magnetic noise and vibrations due to slotting harmonics. He should then check if the slot combination do not create other strong vibrations due to saturation [16]. Finally, he should choose the slot opening widths in order to cancel the identified exciting force harmonics which are left according to [21].

TABLE IV
QUIETEST SLOT COMBINATIONS FOR TEST MOTOR (IN INCREASING NOISE LEVEL ORDER).

Z_s	Z_r
10	40, 20, 30, 50, 15, 25
11	22, 33, 44, 42, 46, 21
12	48, 16, 20, 32, 24, 28, 36, 40, 44
13	39, 15, 43, 35, 48, 50, 49
14	21, 42, 28, 35, 49
15	30, 45, 13, 41
16	12, 20, 24, 28, 32, 36, 40, 44, 48
17	34, 15, 19, 47, 38
18	27, 36, 45, 47, 16
19	38, 25, 34, 22
20	12, 16, 32, 24, 28, 36, 44, 48, 40
21	42, 14, 28, 35
22	11, 25, 19, 35, 31, 44
23	50, 27, 30, 19
24	12, 16, 20, 32, 28, 44, 40, 36, 48
25	32, 21, 33, 29, 46, 44
26	13, 39
27	18, 36, 45, 50, 37, 31
28	12, 16, 20, 24, 32, 36, 40, 44, 48
29	25, 33, 18, 23, 40
30	15, 10, 45, 43, 41, 20
31	41, 27, 25, 50, 35
32	28, 12, 36, 20, 16, 24, 40, 44, 48
33	11, 27, 37, 29, 43, 46
34	17, 19, 15, 49, 45, 30, 38
35	13, 21, 28, 39, 47, 49, 42
36	48, 16, 12, 20, 32, 40, 24, 28, 44
37	33, 30, 31, 11, 49, 50
38	19, 31, 42, 17, 34, 50
39	13, 26, 35, 43, 31, 50
40	12, 32, 16, 44, 24, 36, 28, 20, 48
41	33, 35, 15, 45, 49, 32
42	21, 14, 28, 49, 35
43	25, 30, 47, 35, 39, 13, 15
44	12, 16, 36, 20, 48, 28, 32, 24, 40
45	15, 27, 18, 36, 30, 49
46	21, 37, 25, 50, 39, 13
47	29, 43, 17, 39, 18, 30, 41
48	12, 20, 16, 40, 28, 36, 44, 32, 24
49	14, 21, 42, 39, 28, 35, 41
50	40, 41, 31, 23, 20, 44, 28

V. CONCLUSION

The phenomenon of magnetic noise and vibrations due to slotting harmonics has been analytically demonstrated, as well as the strong influence of rotor and stator slot numbers. An analytical rule to avoid magnetic noise has been established, but it is rather hard to be used in practical by motor designers.

A fully analytical model of an induction machine vibro-acoustic behavior has been therefore presented. On the ground of this model that has been validated at different stages, several simulations have been run in order to exhaustively explore the slot numbers combination impact on variable-speed noise. These simulations have been run with special care, so that results only reflect the effect of slot numbers on noise, independently of the slot geometries.

From these simulations, some low-noise combinations have been clearly established on a 700 W induction machine. These results can be easily used by designers for motors with similar natural frequencies.

REFERENCES

[1] G. Kron, “Induction motor slot combinations: rules to predetermine crawling vibration, noise and hooks in the speed-torque curve,” *AIEE Transactions*, vol. 50, 1931.

[2] P. Timar, *Noise and vibration of electrical machines*. Elsever, 1989.

[3] J. Le Besnerais, A. Fasquelle, M. Hecquet, V. Lanfranchi, P. Brochet, and A. Randria, “A fast noise-predictive multiphysical model of the PWM-controlled induction machine,” in *Proc. of the International Conference on Electrical Machines (ICEM’06)*, (Chania, Greece), July 2006.

[4] J. Le Besnerais, V. Lanfranchi, M. Hecquet, P. Brochet, and G. Friedrich, “Acoustic noise of electromagnetic origin in a fractional-slot induction machine,” *COMPEL*, vol. 27, pp. 1033 – 1052, Feb. 2008.

[5] A. Belhacen, “Vibrations of rotating electrical machines due to magnetomechanical coupling and magnetostriction,” *IEEE Trans. on Magnetics*, vol. 42, Apr. 2006.

[6] T. Hilgert, A. Vandevelde, and J. Melkebeek, “Numerical analysis of the contribution of magnetic forces and magnetostriction to the vibrations in induction machines,” *IET Sci. Meas. Technol.*, vol. 1, no. 1, 2007.

[7] A. Belahcen, *Magnetoelasticity, magnetic forces and magnetostriction in electrical machines*. PhD thesis, Helsinki University of Technology, Finland, Aug. 2004.

[8] P. Alger, *Induction machines : their behaviour and uses*. Gordon and Breach Science Publishers, 1970.

[9] H. Jordan, *Electric motor silencer - formation and elimination of the noises in the electric motors*. W. Giradet-Essen editor, 1950.

[10] S. J. Yang, *Low noise electrical motors*. Oxford: Clarendon Press, 1981.

[11] W. Soedel, *Vibrations of shells and plates*. Marcel Dekker, 1993.

[12] S. Verma and A. Balan, “Determination of radial-forces in relation to noise and vibration problems of squirrel-cage induction motors,” *IEEE Trans. on En. Conv.*, vol. 9, pp. 404–412, June 1994.

[13] J. Le Besnerais, *Reduction of magnetic noise in PWM-supplied induction machines – low-noise design rules and multi-objective optimisation*. PhD thesis, Ecole Centrale de Lille, France, Nov. 2008.

[14] G. Bossio, C. D. Angelo, J. Solsona, G. Garcia, and M. Valla, “A 2-D model of the induction machine: an extension of the modified winding function approach,” *IEEE Trans. on Energy Conversion*, vol. 19, pp. 62–67, Mar. 2004.

[15] J. Brudny, “Modélisation de la denture des machines asynchrones : phénomènes de résonances,” *Journal of Physics III*, vol. 37, no. 7, pp. 1009–1023, 1997.

[16] J. Le Besnerais, V. Lanfranchi, M. Hecquet, G. Lemaire, E. Augis, and P. Brochet, “Charaterization and reduction of magnetic noise due to saturation in induction machines,” *IEEE Trans. on Mag.* Accepted for publication.

[17] P. Timar and J. Lai, “Acoustic noise of electromagnetic origin in an ideal frequency-converter-driven induction motor,” *IEE Proc. on Electr. Power Appl.*, vol. 141, pp. 341–346, Nov. 1994.

[18] J. Le Besnerais, V. Lanfranchi, M. Hecquet, P. Brochet, and G. Friedrich, “Characterisation of the radial vibration force and vibration behaviour of a PWM-fed fractional-slot induction machine,” *IET Electric Power Applications*, Feb. 2009.

[19] J. Le Besnerais, V. Lanfranchi, M. Hecquet, and P. Brochet, “Characterization of the audible magnetic noise emitted by traction motors in railway rolling stock,” in *Proc. of the INTERNOISE conference*, (Shanghai, China), Oct. 2008.

[20] I. Boldea and S. A. Nasar, *The induction machine handbook*. CRC Press, 2002.

[21] J. Le Besnerais, V. Lanfranchi, M. Hecquet, and P. Brochet, “Optimal slot opening width for magnetic noise reduction in induction motors,” *IEEE Trans. on En. Conv.* Accepted for publication.